HHS Public Access

Author manuscript

Neurosci Lett. Author manuscript; available in PMC 2020 February 24.

Published in final edited form as:

Neurosci Lett. 2009 January 30; 450(2): 176–180. doi:10.1016/j.neulet.2008.11.025.

DIFFERENTIAL ACTIVATION OF RAC1 AND RHOA IN NEUROBLASTOMA CELL FRACTIONS

Jennifer L. Seifert, **Sonyta Som**, **DiAnna L. Hynds***

Department of Biology, Texas Woman's University, Denton TX 76204-5799

Abstract

The Rho guanine nucleotide triphosphatases (GTPases) Rac1 and RhoA are important regulators of axon growth. However, the specific roles each plays are complicated by implications that each is involved in promoting and inhibiting neurite outgrowth. Differential regulation of Rac1 and RhoA activation in cell bodies and growth cones may be important in directing axon growth. To test this, we separated neuroblastoma cells into growth cone and cell body fractions and assessed Rac1 and RhoA activation in response to outgrowth promoters, serum withdrawal and 8-bromoadeosine-5′3′-cyclic monophosphate (8-Br-cAMP), and outgrowth inhibitors, chondroitin sulfate proteoglycans (CSPGs) or semaphorin 3A (Sema 3A). In whole cell lysates, serum withdrawal decreased and CSPGs or Sema 3A increased RhoA activity, but no treatments affected Rac1 activity. In growth cones, serum withdrawal or 8-Br-cAMP increased Rac1 activation and serum withdrawal decreased RhoA activation. Conversely, outgrowth inhibitors decreased Rac1 activity. Additionally, 8-Br-cAMP reversed increases in RhoA activity induced by Sema 3A in whole cell lysates and CSPGs in growth cones. These data suggest that activation of RhoA and Rac1 is differentially regulated in specific cellular regions, perhaps contributing to the complexity of Rho GTPase-mediated axon growth.

Keywords

Axon growth; Chondroitin sulfate proteoglycans; Cyclic AMP analogs; Growth cones; Rho GTPases; Semaphorin 3A

Axon extension is guided by environmental cues [9], many of which signal through Rho GTPases. In non-neuronal cells, activation of RhoA, Rac1 and Cdc42 results in the formation of stress fibers, lamellipodia and filopodia, respectively [11]. In neurons, functional studies of Rho GTPase function assess the effects of guidance cues on their activity and the effects of manipulating their activation on neurite outgrowth. Generally, outgrowth promoters activate Rac1 and Cdc42, and inhibitors activate RhoA. For instance, outgrowth promoters like laminin [38], trophic factors [22] and netrins [35] increase Rac1 and/or Cdc42 activation. Outgrowth inhibitors like semaphorins [37] and chondroitin sulfate proteoglycans (CSPGs) [5] increase RhoA activation. Dominant active RhoA generally leads

Correspondence: DiAnna L. Hynds, Ph.D., PO Box 425799, Denton, TX 76204-5799, Office: 940-898-2359, Fax: 940-898-2382, DHynds@twu.edu.

to outgrowth inhibition [34], while dominant active Rac1 and Cdc42 lead to increased extension [6, 32].

However, manipulating Rho GTPase activation or signaling has yielded unexpected results from some experiments. For example, lysophosphatidic acid induced RhoA activation inhibits outgrowth [16]. However, inhibiting RhoA (or Rho associated kinase) demonstrated its necessity for axon navigation [14]. Additionally, Rac1 activity is required for outgrowth [19], but dominant active or dominant negative Rac1 decreases extension [18]. These disparities persist in more mechanistic studies showing RhoA activity is needed for growth cone consolidation and efficient migration [20] and Rac1 activation is linked to growth cone retractions [15].

One potential explanation for these different results could be compartmentalization of Rho GTPase activation. In fluorescence resonance energy transfer (FRET) studies [1, 25], RhoA and Rac1 were active in the peripheral domains of growth cones, while RhoA was also active in axon shafts and central domains. RhoA activation in axon shafts resulted in retraction and activation in the peripheral domain was necessary for growth cone spreading [25]. These studies implicate compartmentalization as a potential regulatory mechanism, but FRET results depend on the nature of the probe and can be difficult to interpret.

Here, we investigated the subcellular compartmentalization of Rho GTPase activity in a physiological context. We separated growth cones and cell bodies of B35 rat neuroblastoma cells (ATCC, Manassas, VA) using differential centrifugation, confirming efficient separation with the growth cone marker 2G13p [2, 36] and the nuclear marker lamin B. We treated cells with the outgrowth promoters serum withdrawal and 8-Br-cAMP (10 μM, Sigma, St. Louis, MO) [28, 33], or the outgrowth inhibitors CSPGs (5 μg/ml, Chemicon, Temecula, CA) and Sema 3A (50 ng/ml, R&D Systems, Minneapolis, MN) [12, 29] and assessed activation of Rac1 or RhoA in growth cone-enriched fractions and whole cell lysates, using pull-down assays and enzyme linked immunosorbance, respectively.

For 2G13 immunocytochemistry, B35 cells (5,000 cells/cm^2) were plated on glass coverslips for 24 hours in Dulbecco's Modified Eagle's Medium (Invitrogen, Carlsbad, CA) containing 10% fetal bovine serum (Sigma, St. Louis, MO), hereafter referred to as serum-containing medium (SCM). Cultures were serum-starved for 24 hours, fixed in 4.0% paraformaldehyde, and washed with phosphate buffered saline (PBS). Samples were blocked in PBS containing 1.5% normal goat serum (Jackson Laboratories, West Grove, PA), 0.1% bovine serum albumin (Fisher, Pittsburgh, PA) and 0.1% Triton X-100 (Sigma, St. Louis, MO). Samples were incubated overnight at 4.0 °C with mouse 2G13 antibodies (1:500; AbCam, Cambridge, MA), washed with PBS, and incubated with goat anti-mouse AlexaFluor 488-conjugated secondary antibodies (1:200; Invitrogen, Carlsbad, CA) for 1 hour at room temperature. Coverslips were washed in PBS and mounted on slides (Vector Laboratories, Burlingame, CA). Phase contrast and fluorescence images were captured with an AxioVision MrM camera through a 40X objective (N.A. = 0.6) using AxioVision image analysis software (Zeiss, Thornwood, NY).

Growth cone-enriched cell fractions were obtained using differential centrifugation [21]. B35 cells (20,000 cells/cm^2) were grown to 90% confluency in 10 cm plates (BioLink Scientific, Wimberley, TX) and serum-starved for 24 hours. Cells were homogenized in 0.5 mM EDTA, 137 mM NaCl, 10 mM Na_2HPO_4, 2.7 mM KCl, and 0.15 mM KH_2PO_4 (Sigma, St. Louis, MO) and fractionated on 20% sucrose cushions at 500 × *g* for 4 minutes. The putative growth cone and cell body fractions were collected from the sucrose cushion/buffer interface and pellet, respectively. Sucrose was removed by centrifugation (14,000 × *g,* 20 minutes). Each fraction was lysed on ice in 1.0% IGEPAL CA-630, 1.5 mM EDTA, 25 mM Tris-HCl (pH = 7.4), and 150 mM NaCl (Sigma, St. Louis, MO). Each fraction (40 μg total protein; BCA, Pierce, Rockford, IL) was electrophoresed through 15% sodium dodecyl sulfate polyacrylamide gels (SDS/PAGE) and transferred to nitrocellulose (BioRad, Temecula, CA). After blocking in 5% non-fat milk (Fisher, Pittsburgh, PA) in Tris buffered saline containing 0.1% Tween-20 (TBST), membranes were incubated overnight at 4.0°C with 2G13 (1:1000), anti-lamin B (1:500, Calbiochem, La Jolla, CA), anti-actin (1:500, Cytoskeleton, Denver, CO) or anti-α-tubulin (1:500, Invitrogen, Carlsbad, CA). Membranes were washed with TBST and incubated in goat anti-mouse or goat anti-rabbit horseradish peroxidase (HRP)-conjugated secondary antibodies (1:5000; Invitrogen, Carlsbad, CA) for 2 hours at room temperature. Membranes were washed extensively and immunoreactive bands were visualized by enhanced chemiluminescence (ChemiGlow; Alpha Innotech, San Leandro, CA). Coomassie blue-stained sister gels were used to assess protein loading in both fractions.

Rac1 activation in growth cones and whole cell lysates was assessed using pull-down assays. Cells (90% confluent) were maintained in SCM or placed in serum-free medium (SFM) for 24 hours and subsequently treated with outgrowth promoters and inhibitors for 15 minutes. Cells were fractionated and lysed in 1.0% IGEPAL CA-630, 1.5 mM EDTA, 25 mM Tris-HCL (pH = 7.4), and 150 mM NaCl. Growth cone or whole cell lysates (200–400 μg total protein) were incubated with 20 μg p21-activated kinase protein binding domain conjugated agarose beads (Cytoskeleton, Denver, CO) for 45 minutes at 4.0 °C. Beads were washed three times in 25 mM Tris (pH = 7.5), 30 mM $MgCl_2$, and 40 mM NaCl (all from Sigma, St. Louis, MO) and boiled in Laemmli buffer (Sigma, St. Louis, MO). Samples (20–40 μg lysates; entire pull-down) were immunoblotted with mouse (1:500; BD Biosciences, San Jose, CA) or rabbit (1:500; Cell Signaling Technology, Danvers, MA) anti-Rac1. Immunoreactive bands, visualized by enhanced chemiluminescence, were analyzed using a FluorChem HD2 gel analyzer (Alpha Innotech, San Leandro, CA). Band density readings were used to generate a ratio of active to total Rac1. Ratios were subjected to Kruskal-Wallis analysis of variance (ANOVA) and Mann-Whitney U post hoc analyses at $\alpha = 0.05$ (SPSS, Chicago, IL).

RhoA activation in growth cones and whole cell lysates was measured using the Rho G-LISA assay (Cytoskeleton, Denver, CO). Following treatment, cells were fractionated and lysed. Samples (30–50 μg total protein) were loaded onto a rhotekin coated microtiter plate. Plates were incubated with anti-RhoA primary and HRP-conjugated secondary antibodies (supplied with kit). An HRP detection reagent was added and the absorbance of each well was read at 490 nm. Absorbance readings were blank corrected and normalized by input protein concentration. Positive controls (RhoA-Q63L) were included in each assay. Maximal

(A_{490} = 1.19) and minimal (A_{490} = 0.26) absorbance readings for RhoA activation were obtained from GTP and GDP loaded RhoA protein, respectively. Data were analyzed using Kruskal-Wallis ANOVA and Mann-Whitney U post hoc analyses with a significance level of $\alpha = 0.05$.

The antibody 2G13 labeled both growth cone regions and the putative growth cone fraction in B35 cells. Growth cone regions, identified from phase contrast images (Fig. 1A), were highly 2G13 immunoreactive (Fig. 1B). Primary omitted control samples confirmed labeling specificity (data not shown). In immunoblots from fractionated cells, the 37 kDa 2G13p was present primarily in the putative growth cone fraction (Fig. 1C) [2]. Sister Coomassie blue-stained gels showed abundant protein in both fractions (Fig. 1D). Because total protein appeared to be less in the pellet, we estimated the immunoreactivity in the putative growth cone fraction by normalizing densities for immunoreactive bands in each fraction to the sum of Coomassie blue-stained band densities in each fraction (excluding major histones, bottom of the pellet lane). These calculations revealed a more than 11 fold increase in band density for 2G13p in the growth cone fraction compared with the cell body fraction. Additionally, immunoreactivity for the nuclear marker lamin B was evident only in the pellet fraction (Fig. 1E). Western blotting for actin confirmed its abundance in growth cone fractions (Fig. 1F), while a-tubulin was largely restricted from this fraction (Fig. 1G). These results indicate our fractionation protocol yielded samples enriched for growth cones.

We determined Rac1 activation ratios in whole cell lysates (Fig. 2A) and growth cone fractions (Fig. 2B). In whole cell lysates, no treatments significantly affected Rac1 activation (Fig. 2C, black bars). In particular, serum withdrawal or treatment with 8-Br-cAMP, both reported to promote outgrowth from B35 cells [28, 33], did not increase Rac1 activity. Likewise, CSPGs or Sema 3A did not affect Rac1 activation. In growth cones, SFM increased and CSPGs decreased Rac1 activation (Fig. 2C, white bars). Here, serum withdrawal or 8-Br-cAMP increased Rac1 activation compared SCM. However, treatment with 8-Br-cAMP did not increase Rac1 activation levels above SFM. Treatment with CSPGs or Sema 3A returned Rac1 activation levels to SCM levels. Co-treatment with CSPGs or Sema 3A and 8-Br-cAMP did not alter the inhibition of Rac1 activation by these outgrowth inhibitors. Thus, outgrowth promoters increased and outgrowth inhibitors decreased Rac1 activation in growth cones, but not in whole cells, indicating regulation of Rac1 in growth cones may be masked when assessed using whole cell lysates.

We next determined whether RhoA activation was altered in B35 cell fractions in response to outgrowth promoters or inhibitors. In whole cell lysates, RhoA was activated by Sema 3A and inhibited by serum withdrawal, compared to cells in SCM (Fig. 3, black bars). Compared to SFM, 8-Br-cAMP or outgrowth inhibitors (CSPGs or Sema 3A) increased RhoA activation. Interestingly, co-treatment with Sema 3A and 8-Br-cAMP decreased the RhoA activation observed with either treatment alone. In growth cones, RhoA activation was inhibited by serum withdrawal and increased by 8-Br-cAMP, compared to cells maintained in SCM (Fig. 3, white bars). Compared to serum-starved cells, 8-Br-cAMP increased RhoA activation, while CSPGs or Sema 3A did not. The RhoA activation elicited by 8-Br-cAMP was reversed when cells were co-treated with CSPGs. These data may indicate differential

regulation of RhoA activity in growth cones compared to whole cell lysates or that cAMP and outgrowth inhibitor pathways interactions differently in distinct cell regions.

These results suggest there is significant compartmentalization of Rho GTPase activity in neuron-like cells. Rac1 activity was only affected in growth cones, while RhoA activity was altered both in growth cones and whole cell lysates. We were only able to assess Rho GTPase activity in these fractions. However, our data reinforce those obtained using FRET, where activation of specific Rho GTPases differed in distinct growth cone regions. Exactly how differential regulation of Rho GTPase activity occurs is unclear, but may result from neuronal cyto-architecture or localization of Rho GTPase activators, guanine nucleotide exchange factors (GEFs). In neurons, long axons create a separation between growth cones and cell bodies. Thus, even though receptors for outgrowth promoters (e.g. neurotrophins, netrins) or inhibitors (e.g. the Sema 3A receptor neuropilin-1) are uniformly distributed throughout the cell [17, 27, 30], tissue-specific guidance cue distribution may affect only growth cones. Studies using compartmented cultures, where distal axons and cell bodies are subjected to local cues, support this idea. For example, local application of nerve growth factor to distal axons, but not the cell bodies, is sufficient to maintain axon growth [7]. Directly assessing Rho GTPase function, antagonizing RhoA at cell bodies or distal axons was sufficient to promote outgrowth on inhibitory substrata [4]. However, we show here that compartmentalized regulation of Rho GTPase activity occurs even when the entire cell is exposed to guidance cues. Selective distribution or activation of GEFs might explain regional GTPase activity. In non-neuronal *C. elegans* cells, polarization cues lead to uneven distribution of GET-2, a RHO-1 GEF, and redistribution of RHO-1 and CDC42 [23]. Similarly, RhoA is redistributed in polarized neutrophils by activation of PDZRhoGEF [39]. However, in our cultures, Rho GTPase immunostaining is uniform under a variety of conditions (data not shown), suggesting GEF redistribution may be important. The RhoGEF, Lfc, is non-uniformly distributed in cortical neurons [24]. Experiments in neurons assessing GEF distribution and the effects of manipulating Rho GTPase activity in compartmented cultures may help define axon growth mechanisms.

There may also be spatially-regulated interactions in signaling networks, exemplified here by the regional specificity of cAMP signaling. We found 8-Br-cAMP activation of RhoA in growth cones and whole cell lysates, but it only activated Rac1 in growth cones. Interestingly, 8-Br-cAMP and CSPG co-treatment reversed increases in RhoA activity in growth cones, but 8-Br-cAMP/Sema 3A co-treatment decreased the 8-Br-cAMP-induced increase in RhoA activation in cell bodies. In whole cells, cAMP interactions with Rho GTPases and outgrowth inhibitors are well documented. Increased cAMP activates Rac1 and inhibits RhoA [3]. Out results differ from these since 8-Br-cAMP increased RhoA activity, but agree with other studies [8] showing antagonism between cAMP and Sema 3A. Thus, our results might reflect differences in treatment conditions or crosstalk between different Rho GTPases.

Rho GTPase crosstalk may regulate axon growth with our data indicating the activation of Rac1 relative to RhoA as an important determinant. Using a SCM baseline, we set the ratio of active Rac1 to active RhoA to one. In growth cones, SFM or 8-Br-cAMP increased this ratio to 5.53 and 7.44, respectively. Changes in these ratios in whole cell lysates were

minimal (SFM = 1.11, 8-Br-cAMP = 1.77). CSPGs or Sema 3A produced more pronounced effects in whole cell lysates, where active Rac1:active RhoA was 0.50 and 0.76, respectively. This balance of Rho GTPase activity may determine growth cones advance, but Rho GTPase crosstalk may complicate this scenario, exemplified by inconsistent experimental results. In fibroblasts, Cdc42 activates Rac1 which activates RhoA [26]. However, Rac1 and RhoA antagonize each other's activities in neurons [40] and non-neuronal [31] cells. Interestingly, both Rac1 and RhoA are activated in Sema 3A-mediated growth cone collapse [10, 15]. Mathematical models of Rho GTPase crosstalk [13] may help direct studies investigating Rho GTPase action in different cell types. In summary, we show here that Rac1 and RhoA activity are compartmentally regulated in neuron-like cells, potentially explaining different outcomes from previous work and helping define mechanisms of axon growth.

Acknowledgments

Supported by grants from NIH/NIGMS (R25GM055380) and the TWU Research Enhancement Program, the TWU Chancellor's Research Fellows Program and the Department of Biology. The authors thank Dr. Lynda Uphouse for critically reading an early version of this manuscript.

References

1. Aoki K, Nakamura T, Matsuda M. Spatio-temporal regulation of Rac1 and Cdc42 activity during nerve growth factor-induced neurite outgrowth in PC12 cells. J Biol Chem. 2792004; :713–9. [PubMed: 14570905]
2. Baloui H, von Boxberg Y, Vinh J, Weiss S, Rossier J, Nothias F, Stettler O. Cellular prion protein/laminin receptor: distribution in adult central nervous system and characterization of an isoform associated with a subtype of cortical neurons. Eur J Neurosci. 202004; :2605–16. [PubMed: 15548204]
3. Bandtlow CE. Regeneration in the central nervous system. Exp Gerontol. 382003; :79–86. [PubMed: 12543264]
4. Bertrand J, Winton MJ, Rodriguez-Hernandez N, Campenot RB, McKerracher L. Application of Rho antagonist to neuronal cell bodies promotes neurite growth in compartmented cultures and regeneration of retinal ganglion cell axons in the optic nerve of adult rats. J Neurosci. 252005; :1113–21. [PubMed: 15689547]
5. Borisoff JF, Chan CC, Hiebert GW, Oschipok L, Robertson GS, Zamboni R, Steeves JD, Tetzlaff W. Suppression of Rho-kinase activity promotes axonal growth on inhibitory CNS substrates. Mol Cell Neurosci. 222003; :405–16. [PubMed: 12691741]
6. Brown MD, Cornejo BJ, Kuhn TB, Bamburg JR. Cdc42 stimulates neurite outgrowth and formation of growth cone filopodia and lamellipodia. J Neurobiol. 432000; :352–64. [PubMed: 10861561]
7. Campenot RB. NGF and the local control of nerve terminal growth. J Neurobiol. 251994; :599–611. [PubMed: 8071664]
8. Chalasani SH, Sabelko KA, Sunshine MJ, Littman DR, Raper JA. A chemokine, SDF-1, reduces the effectiveness of multiple axonal repellents and is required for normal axon pathfinding. J Neurosci. 232003; :1360–71. [PubMed: 12598624]
9. Chilton JK. Molecular mechanisms of axon guidance. Dev Biol. 2922006; :13–24. [PubMed: 16476423]
10. Dontchev VD, Letourneau PC. Nerve growth factor and semaphorin 3A signaling pathways interact in regulating sensory neuronal growth cone motility. J Neurosci. 222002; :6659–69. [PubMed: 12151545]
11. Hall A. Rho GTPases and the control of cell behaviour. Biochem Soc Trans. 332005; :891–5. [PubMed: 16246005]

12. Hynds DL, Snow DM. Neurite outgrowth inhibition by chondroitin sulfate proteoglycan: stalling/stopping exceeds turning in human neuroblastoma growth cones. Exp Neurol. 1601999; :244–55. [PubMed: 10630209]
13. Jilkine A, Maree AF, Edelstein-Keshet L. Mathematical model for spatial segregation of the Rho-family GTPases based on inhibitory crosstalk. Bull Math Biol. 692007; :1943–78. [PubMed: 17457653]
14. Jin K, Mao XO, Greenberg DA. Vascular endothelial growth factor stimulates neurite outgrowth from cerebral cortical neurons via Rho kinase signaling. J Neurobiol. 662006; :236–42. [PubMed: 16329123]
15. Jin Z, Strittmatter SM. Rac1 mediates collapsin-1-induced growth cone collapse. J Neurosci. 171997; :6256–63. [PubMed: 9236236]
16. Kranenburg O, Poland M, van Horck FP, Drechsel D, Hall A, Moolenaar WH. Activation of RhoA by lysophosphatidic acid and Galpha12/13 subunits in neuronal cells: induction of neurite retraction. Mol Biol Cell. 101999; :1851–7. [PubMed: 10359601]
17. Kryl D, Yacoubian T, Haapasalo A, Castren E, Lo D, Barker PA. Subcellular localization of full-length and truncated Trk receptor isoforms in polarized neurons and epithelial cells. J Neurosci. 191999; :5823–33. [PubMed: 10407023]
18. Kuhn TB, Brown MD, Bamburg JR. Rac1-dependent actin filament organization in growth cones is necessary for beta1-integrin-mediated advance but not for growth on poly-D-lysine. J Neurobiol. 371998; :524–40. [PubMed: 9858256]
19. Li X, Saint-Cyr-Proulx E, Aktories K, Lamarche-Vane N. Rac1 and Cdc42 but not RhoA or Rho kinase activities are required for neurite outgrowth induced by the Netrin-1 receptor DCC (deleted in colorectal cancer) in N1E-115 neuroblastoma cells. J Biol Chem. 2772002; :15207–14. [PubMed: 11844789]
20. Loudon RP, Silver LD, Yee HF Jr, Gallo G. RhoA-kinase and myosin II are required for the maintenance of growth cone polarity and guidance by nerve growth factor. J Neurobiol. 662006; :847–67. [PubMed: 16673385]
21. Meyerson G, Pfenninger KH, Pahlman S. A complex consisting of pp60c-src/pp60c-srcN and a 38 kDa protein is highly enriched in growth cones from differentiated SH-SY5Y neuroblastoma cells. J Cell Sci. 103(Pt 1)1992; :233–43. [PubMed: 1385459]
22. Miyamoto Y, Yamauchi J, Tanoue A, Wu C, Mobley WC. TrkB binds and tyrosine-phosphorylates Tiam1, leading to activation of Rac1 and induction of changes in cellular morphology. Proc Natl Acad Sci U S A. 1032006; :10444–9. [PubMed: 16801538]
23. Motegi F, Sugimoto A. Sequential functioning of the ECT-2 RhoGEF, RHO-1 and CDC-42 establishes cell polarity in Caenorhabditis elegans embryos. Nat Cell Biol. 82006; :978–85. [PubMed: 16921365]
24. Muly EC, Nairn AC, Greengard P, Rainnie DG. Subcellular distribution of the Rho-GEF Lfc in primate prefrontal cortex: effect of neuronal activation. J Comp Neurol. 5082008; :927–39. [PubMed: 18399541]
25. Nakamura T, Aoki K, Matsuda M. FRET imaging in nerve growth cones reveals a high level of RhoA activity within the peripheral domain. Brain Res Mol Brain Res. 1392005; :277–87. [PubMed: 16024133]
26. Nobes CD, Hall A. Rho, rac, and cdc42 GTPases regulate the assembly of multimolecular focal complexes associated with actin stress fibers, lamellipodia, and filopodia. Cell. 811995; :53–62. [PubMed: 7536630]
27. Osborne PB, Halliday GM, Cooper HM, Keast JR. Localization of immunoreactivity for deleted in colorectal cancer (DCC), the receptor for the guidance factor netrin-1, in ventral tier dopamine projection pathways in adult rodents. Neuroscience. 1312005; :671–81. [PubMed: 15730872]
28. Otey CA, Boukhelifa M, Maness P. B35 neuroblastoma cells: an easily transfected, cultured cell model of central nervous system neurons. Methods Cell Biol. 712003; :287–304. [PubMed: 12884695]
29. Puschel AW, Adams RH, Betz H. Murine semaphorin D/collapsin is a member of a diverse gene family and creates domains inhibitory for axonal extension. Neuron. 141995; :941–8. [PubMed: 7748561]

30. Reza JN, Gavazzi I, Cohen J. Neuropilin-1 is expressed on adult mammalian dorsal root ganglion neurons and mediates semaphorin3a/collapsin-1-induced growth cone collapse by small diameter sensory afferents. Mol Cell Neurosci. 141999; :317–26. [PubMed: 10588387]
31. Sander EE, ten Klooster JP, van Delft S, van der Kammen RA, Collard JG. Rac downregulates Rho activity: reciprocal balance between both GTPases determines cellular morphology and migratory behavior. J Cell Biol. 1471999; :1009–22. [PubMed: 10579721]
32. Sarner S, Kozma R, Ahmed S, Lim L. Phosphatidylinositol 3-kinase, Cdc42, and Rac1 act downstream of Ras in integrin-dependent neurite outgrowth in N1E-115 neuroblastoma cells. Mol Cell Biol. 202000; :158–72. [PubMed: 10594018]
33. Schubert D, Heinemann S, Carlisle W, Tarikas H, Kimes B, Patrick J, Steinbach JH, Culp W, Brandt BL. Clonal cell lines from the rat central nervous system. Nature. 2491974; :224–7. [PubMed: 4151463]
34. Sebok A, Nusser N, Debreceni B, Guo Z, Santos MF, Szeberenyi J, Tigyi G. Different roles for RhoA during neurite initiation, elongation, and regeneration in PC12 cells. J Neurochem. 731999; :949–60. [PubMed: 10461884]
35. Shekarabi M, Kennedy TE. The netrin-1 receptor DCC promotes filopodia formation and cell spreading by activating Cdc42 and Rac1. Mol Cell Neurosci. 192002; :1–17. [PubMed: 11817894]
36. Stettler O, Bush MS, Kasper M, Schlosshauer B, Gordon-Weeks PR. Monoclonal antibody 2G13, a new axonal growth cone marker. J Neurocytol. 281999; :1035–44. [PubMed: 11054903]
37. Swiercz JM, Kuner R, Behrens J, Offermanns S. Plexin-B1 directly interacts with PDZ-RhoGEF/LARG to regulate RhoA and growth cone morphology. Neuron. 352002; :51–63. [PubMed: 12123608]
38. Weston CA, Anova L, Rialas C, Prives JM, Weeks BS. Laminin-1 activates Cdc42 in the mechanism of laminin-1-mediated neurite outgrowth. Exp Cell Res. 2602000; :374–8. [PubMed: 11035933]
39. Wong K, Van Keymeulen A, Bourne HR. PDZRhoGEF and myosin II localize RhoA activity to the back of polarizing neutrophil-like cells. J Cell Biol. 1792007; :1141–8. [PubMed: 18086913]
40. Yamaguchi Y, Katoh H, Yasui H, Mori K, Negishi M. RhoA inhibits the nerve growth factor-induced Rac1 activation through Rho-associated kinase-dependent pathway. J Biol Chem. 2762001; :18977–83. [PubMed: 11279039]

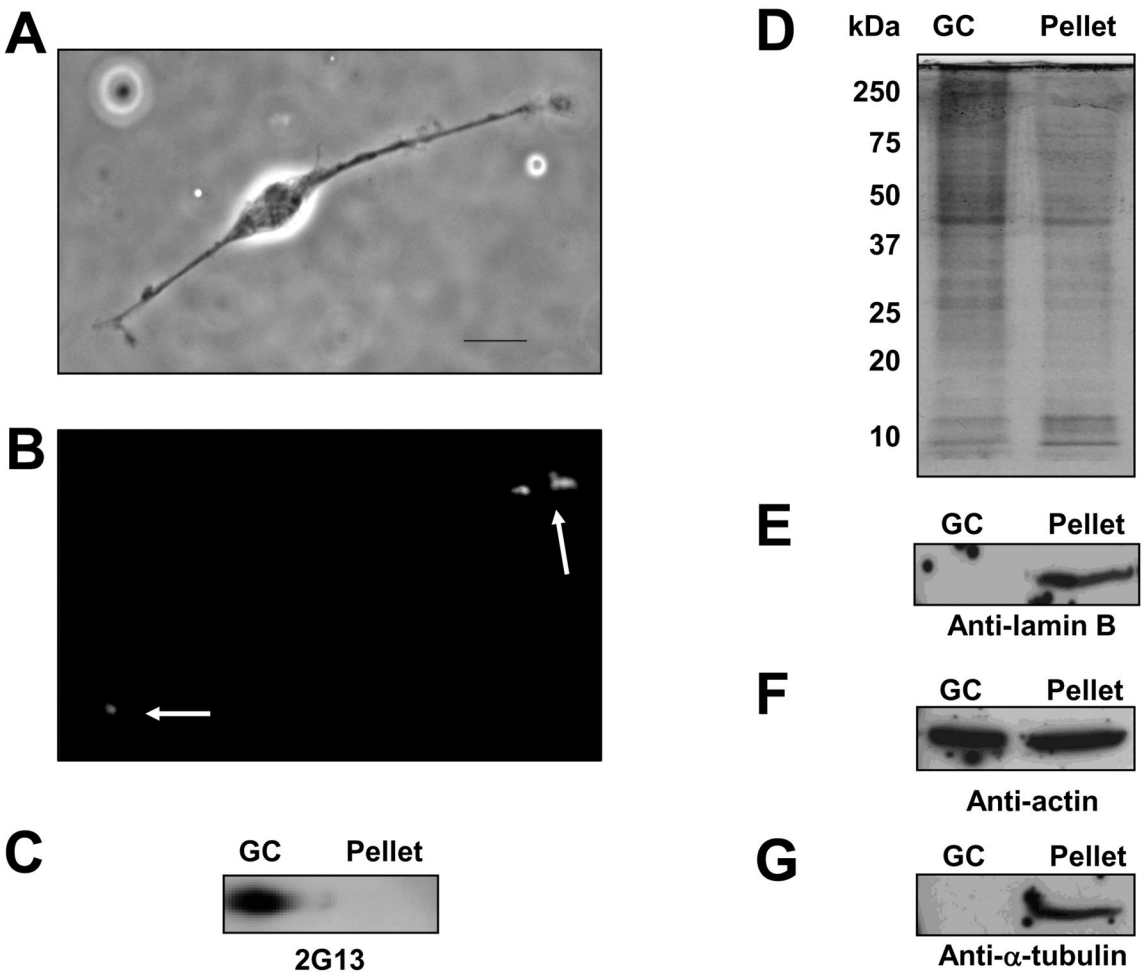

Fig. 1.

Cell fractionation yields a growth cone-enriched fraction. Phase contrast (A) and fluorescent (B) images of B35 cells stained for the growth cone marker, 2G13p. Arrows indicate growth cones. Scale bar = 10 μm. C) Western blot probed with 2G13. GC represents the fraction collected at the sucrose/buffer interface and pellet is the fraction migrating to the bottom of the tube, corresponding to cell bodies. D) Coomassie blue stained gel of lysates from GC and pellet. E) Western blot for lamin B shows this nuclear antigen mainly in the GC fraction. F) Western blot for actin showing abundant actin in the GC and pellet fractions. G) Western blot for α-tubulin showing predominance in pellets.

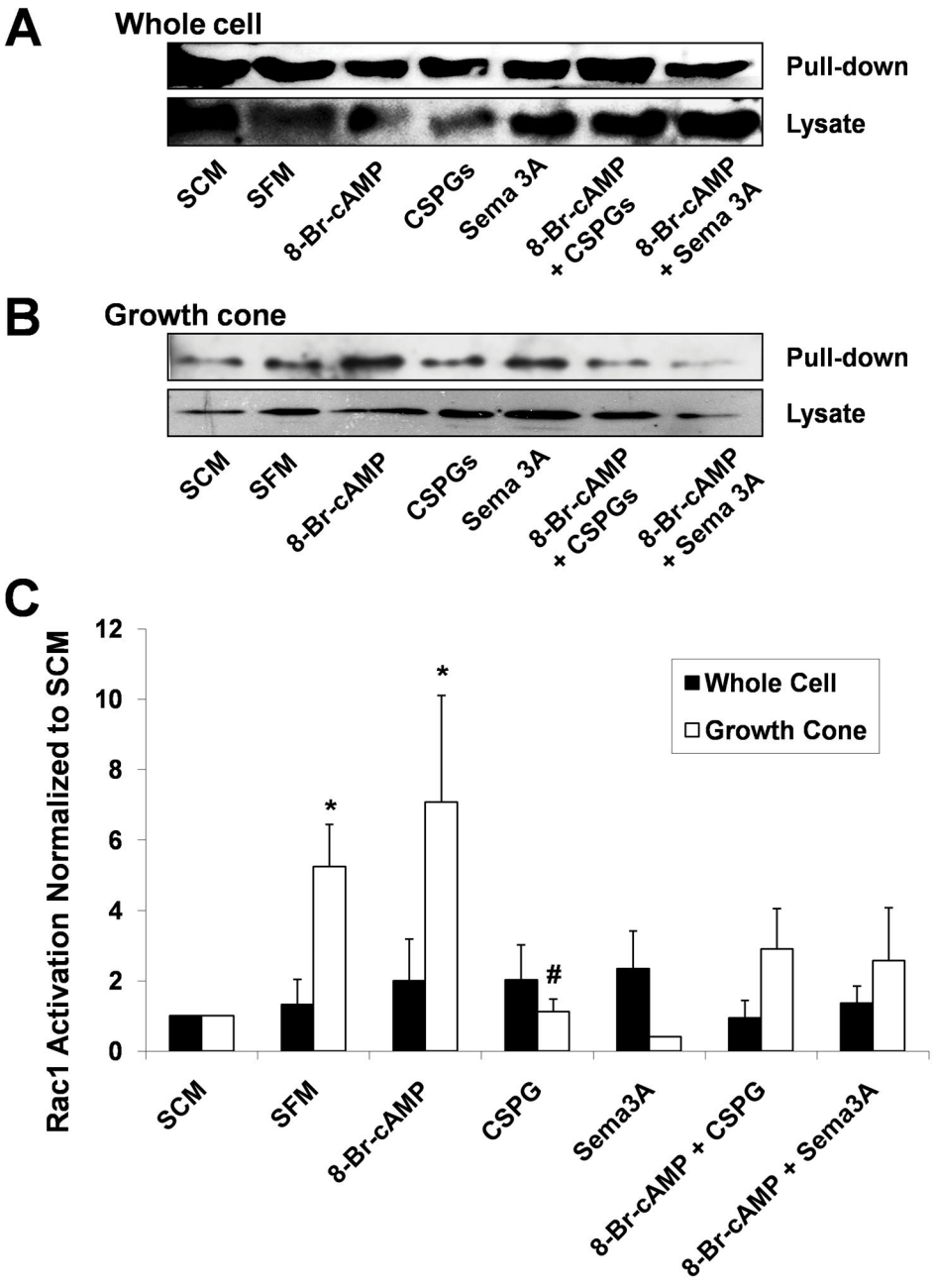

Fig. 2.

Rac1 activation in whole cell lysates and growth cone fractions. A) Rac1 western blot for activated (pull-down, top panel) and total (lysate, bottom panel) Rac1 in whole cells (SCM = serum-containing medium, SFM = serum free medium, 8-Br-cAMP = 10 μM 8-bromoadenosine 5′,3′ cyclic monophosphate, CSPGs = 5 μg/ml chondroitin sulfate proteoglycans, or Sema3A = 50 ng/ml semaphorin 3A). B) Rac1 western blot from growth cone fractions for activated (top panel) and total (bottom panel) Rac1. C) Ratios of active to total Rac1 determined by scanning densitometry normalized to SCM. Data are means + SEM of 4 (whole cell lysates) or 3 (growth cones) experiments. N = 2 for the Sema 3A

condition in the growth cone fraction. Significant differences at $p < 0.05$ (Kruskal-Wallis ANOVA and Mann-Whitney U post hoc) are indicated by * compared to SCM, # compared to SFM, and ^ compared to 8-Br-cAMP.

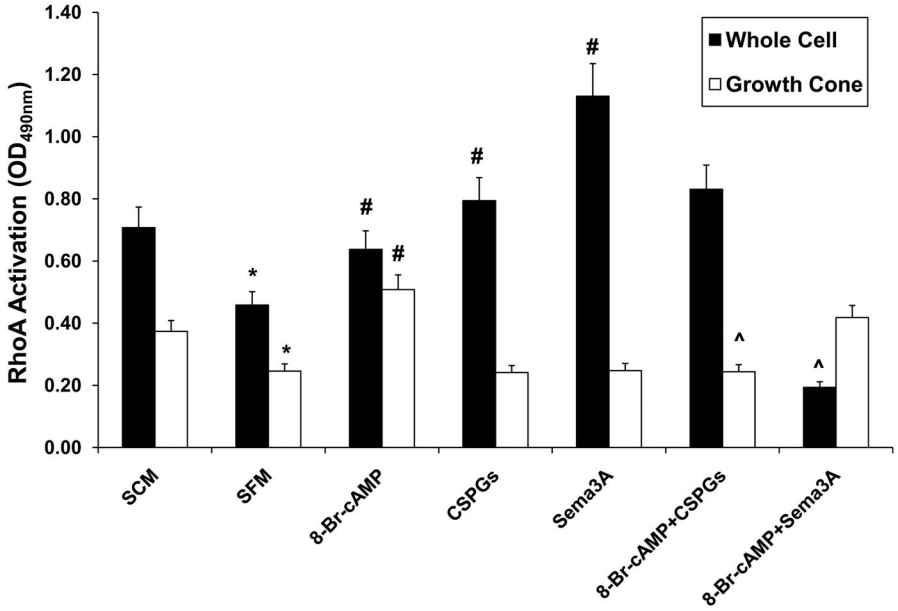

Fig. 3.

RhoA activation in whole cell lysates (black bars) and growth cone fractions (white bars). RhoA activation was assessed using RhoA G-LISA in cells treated with outgrowth promoters or inhibitors (SCM = serum-containing medium, SFM = serum free medium, 8-Br-cAMP = 10 μM 8-bromoadenosine 5′,3′ cyclic monophosphate, CSPGs = 5 μg/ml chondroitin sulfate proteoglycans, or Sema3A = 50 ng/ml semaphorin 3A). Data are means + SEM of absorption at 490 nm, normalized to protein concentration, for 3 experiments. Significant differences at $p<0.05$ (Kruskal-Wallis ANOVA and Mann-Whitney U post hoc) are indicated by * compared to SCM, # compared to SFM and ^ compared to 8-Br-cAMP.